# SUNSET–SUNRISE CHARACTERISTICS OF SPORADIC LAYERS OF IONIZATION IN THE LOWER IONOSPHERE OBSERVED BY THE METHOD OF RESONANCE SCATTERING OF RADIO WAVES FROM ARTIFICIAL PERIODIC INHOMOGENEITIES OF THE IONOSPHERIC PLASMA

**N. V. Bakhmet'eva,* V. V. Belikovich, L. M. Kagan, and A. A. Ponyatov**

UDC 551.510.536

*We present the results of studying the sporadic layers of ionization in the lower ionosphere observed in the sunset–sunrise time during the summer months of 2000 and 2001. Measurements were performed at the "Sura" heating facility of the Radiophysical Research Institute (Nizhny Novgorod, Russia). Based on the analysis of the altitude–time dependences of the amplitude, relaxation time, and phase of the scattered signal, we obtain new data on the formation and dynamics of the evening and nighttime mid-latitude sporadic E layer, present the results of measuring the velocity of the plasma vertical motion, and estimate the relative molecular mass and total number density of metal ions whose pile-up due to the wind shear can cause the formation of the observed sporadic layers.*

## 1. INTRODUCTION

In [1], the results of studying the inhomogeneous structure of the lower ionosphere by the method of artificial periodic inhomogeneities (APIs) have been reported. These results were obtained on the basis of daytime measurements in August 1999. In particular, the brightness records (altitude–time dependences) of the scattered signal and the temporal behavior and altitude profiles of its amplitude and relaxation time were obtained and analyzed. In addition, the altitude–time variations in the atmospheric temperature and density, the velocity of the plasma vertical motion, and the vertical component of the turbulent velocity were studied. Moreover, new data on scattering of radio waves by APIs were presented, various ionospheric formations including sporadic layers and large-scale ionospheric irregularities were identified, and the dynamics of these irregularities as well as the altitudes of their appearance and their temporal characteristics were analyzed. In particular, it was shown that in many cases, the scattered-signal amplitude is determined by interference of waves from APIs and natural ionospheric irregularities. This causes rapid variations in the signal and changes the altitude dependences of its amplitude and relaxation time.

In 2000 and 2001, new evening and nighttime experiments were performed, including the sunset and sunrise times, namely, from 19:00 to 05:00 LT (local time) in August 16 and 17, 2000 (with a break from 22:00 to 02:00 LT) and from 18:00 to 05:30 LT in June 15 and 16, 2001. Note that according to long-term ionospheric observations performed by various methods, the main maximum of probability of the appearance of the sporadic E layer ($E_s$) in the northern hemisphere occurs in June [2], and 80% of annual reflections from the $E_s$ layer are registered from May to August. The purpose of experiments in 2000 was to study the nighttime ionization of the D and E regions, including sporadic layers, by the API method. One of

* nbakh@nirfi.sci-nnov.ru

Radiophysical Research Institute, Nizhny Novgorod, Russia. Translated from Izvestiya Vysshikh Uchebnykh Zavedenii, Radiofizika, Vol. 48, No. 1, pp. 16–32, January 2005. Original article submitted December 16, 2003; accepted October 18, 2004.

 0033-8443/05/4801-0014 

the obtained results was the observation of signals scattered by APIs from the E layer with a maximum amplitude of up to 50 dB after the sunset at the corresponding altitudes, as well as the appearance of these signals before the sunrise. It can be assumed that the signals scattered by APIs and, hence, ionization of the E region existed during the entire night (this was reported in [3]). Another result obtained from the analysis of brightness records of the scattered-signal amplitude and phase was the conclusion that during the sunrise–sunset time, sporadic structures with various spatio-temporal scales are observed in the upper part of the D region and in the lower part of the E region almost constantly. According to observation data of 2000, reflections from these layers can be relatively "smooth" or can have a pronounced "cloudy" structure. These results turned out to be interesting, and the experiment was repeated in June 2001. The observations lasted almost the entire night. The joint results of these two experiments are presented in this paper.

## 2. LAYOUT OF THE EXPERIMENT

The method of study is based on the formation of artificial periodic inhomogeneities of electron number density in the ionosphere in the field of a high-power standing wave from the ground-based radio transmitter, on the probing of APIs by weak signals not perturbing the medium, and on measurements of the amplitude and phase of a backscattered probing signal. The idea of the method consists in that artificial periodic inhomogeneities of the ionospheric plasma arise in the field of a high-power standing wave formed due to interference of a wave incident on the ionosphere and a wave reflected from it. The electron gas is heated in the antinodes of the standing wave, which leads to the formation of a periodic structure with spatial period equal to one half of the wavelength $\lambda$ of the high-power radio wave (Fig. 1*a*). In turn, temperature irregularities form irregularities of electron number density. The formation and relaxation of APIs after switch-off of heating in each ionospheric region are determined by various physical processes including variations in the content, density, and temperature of the atmosphere and in the dissociation and ionization rates with the altitude. This allows one to apply such a method to diagnose the ionosphere [4]. The method of resonance scattering by APIs makes it possible to register signals from comparatively weak inhomogeneities (in the case of a relative density greater than $10^2$).

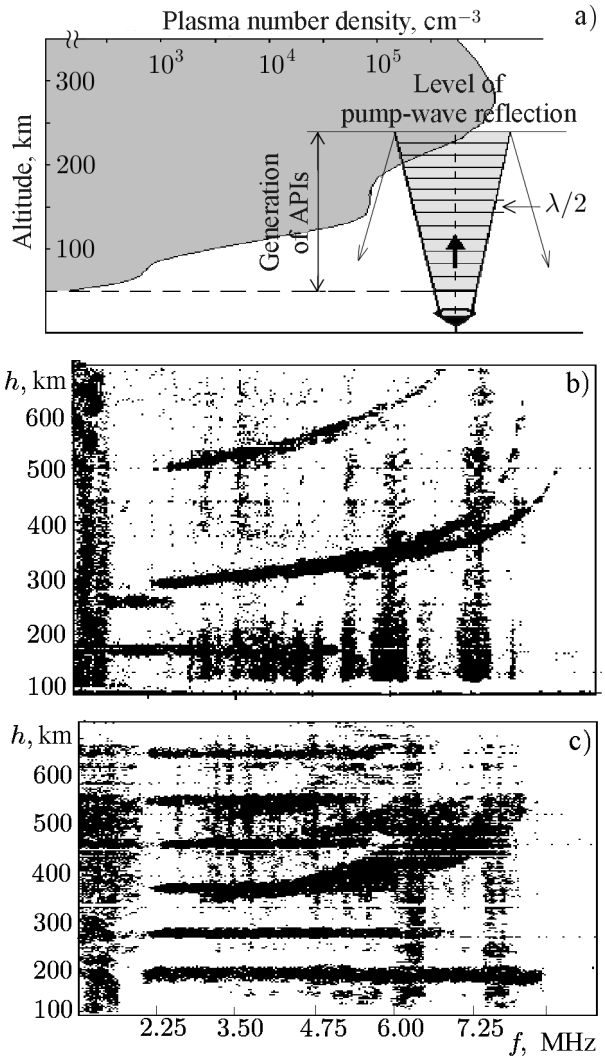


Fig. 1. Diagram showing the formation of artificial periodic inhomogeneities of the ionospheric plasma (*a*) and examples of ionograms at 20:45:00 LT in August 16, 2000 (*b*) and at 23:15:00 LT in June 15, 2001 (*c*).

APIs were created using the "Sura" heating facility (56.1° N and 46.1° E) with an effective radiated power of about 70 and 170 MW in the experiments of 2000 and 2001, respectively. Each session lasted 20 s. During the first 3 s, the ionosphere was heated by an X-polarized radio wave at the frequency $f = 5.67$ MHz. This 3-s heating period was followed by a 17-s pause. Probing pulses with the same frequency, a 25-$\mu$s duration, and a 50 Hz repetition rate were radiated for the first four seconds of the pause. An antenna consisting of 12 in-phase dipoles received scattered X-polarized signals. The signals were amplified by a receiver with a 40-kHz passband. The quadrature components of the scattered signal

were digitized with a step of 1.4 km in altitude and were coded by a 12-bit analog-to-digital converter. Next, the amplitude and phase of the signal were calculated for each altitude. The temporal dependences of these quantities were then approximated by the functions $\ln A(t) = \ln A_0 - t/\tau$ and $\varphi(t) = \varphi_0 + 4\pi Vt/\lambda$. Here, $\lambda$ is the wavelength of the probing wave in the plasma, $\tau$ is the signal relaxation time characterizing the API lifetime after switch-off of heating, and $V$ is the velocity of vertical motion of APIs (see [4] for more details). The natural-noise level amounted to 10–15 dB in various observation times, although time intervals with intense pulse noise took place. Scanning was performed from an altitude of 50 km to the altitude of reflection of a high-power radio wave. In this paper, all the results are given for the lower ionosphere, i.e., for the altitude range 50–120 km.

To monitor the general state of the ionosphere, vertical-sounding ionograms were recorded each 15 min. Examples of two ionograms are shown in Figs. 1*b* and 1*c*.

## 3. AMPLITUDE AND RELAXATION TIME OF THE SCATTERED SIGNAL

### 3.1. Results of observations in August 16 and 17, 2000

Figure 2 shows the brightness records (altitude–time dependences) of the scattered signal for measurements in August 16 and 17, 2000. The dark line shows the altitude dependences of the sunset and sunrise times (left and right panels, respectively) at ionospheric altitudes. The data for the amplitude $A$ and the vertical-motion velocity $V$ are given in the initial form without preliminary processing, whereas the values of the relaxation time $\tau$ are smoothed over the altitude (in a 2.8-km interval) and time (in a 5-min interval). The negative values of $V$ correspond to the upward motion. Figure 2 shows signals from API at altitudes 56–80 and 84–115 km in the D and E regions, respectively.

First of all, we briefly discuss the signals from APIs in the ionospheric D region. Rather weak signals were observed for approximately one hour after the sunset at these altitudes. Then they disappeared and appeared again in approximately 30 min after the sunrise. We emphasize a phenomenon defined in [3] as the sunset–sunrise asymmetry of the altitude–time dependence of the scattered signal. In particular, this asymmetry exhibits itself in that the signals from APIs at the sunset have greater amplitudes and occupy a wider frequency range than at the sunrise, which is well seen in Fig. 2*a*. The altitude range between the D and E regions, from which the scattered signals were not observed, reached 7 and 15 km before the sunset and after the sunrise, respectively. In [3], based on qualitative analysis and numerical calculations of the relaxation time and the amplitude of the scattered signal within the framework of a model of aeronomic processes with a single negative ion, it is shown that these features stem from an increase in the electron detachment rate due to enhanced atomic-oxygen concentration. Note that the temperature dependence of the coefficient of electron attachment to neutral molecules plays the main role in the formation of APIs in the D region [4].

According to the ionosonde data, the cutoff frequencies of the E region amounted to 2.0–2.5 MHz. A semitransparent $E_s$ layer with the blanketing frequency $f_b$ = 1.5–3.0 MHz and the cutoff frequency $f_0$ = 1.5–5.0 MHz is seen in the ionograms. Signals from APIs in the E region were observed during the entire measurement time. Sporadic signals of typical form are also seen in the brightness records of each session. Since the $E_s$ layer was observed in the ionograms in this time (Fig. 1*b*), these signals could be related to scattering by irregularities of the semitransparent sporadic E layer. Two distinguished altitude intervals with the maximum amplitude of the scattered signal are well seen near 92 and 106 km in the E region on the left panel in Fig. 2*a*. The amplitude of these signals reached 55 dB and the relaxation time significantly (by a factor of up to 5) exceeded values typical of the APIs in the E region (0.5–2.5 s). Near the first altitude, a well pronounced thin layer of ionization, which often had a "cloudy" structure, existed almost all the time. Such sporadic clouds of ionization are well seen in 3-s "snapshots" of resonance scattering in Fig. 3. The amplitude of the signal at the "cloud" center can be 10–40 dB greater than that near the boundaries. As a rule, the duration $\xi$ of the "clouds" amounted to about 0.5–2.0 s.

At altitudes above 96 km, reflections from the lower layer gradually went into reflections from the

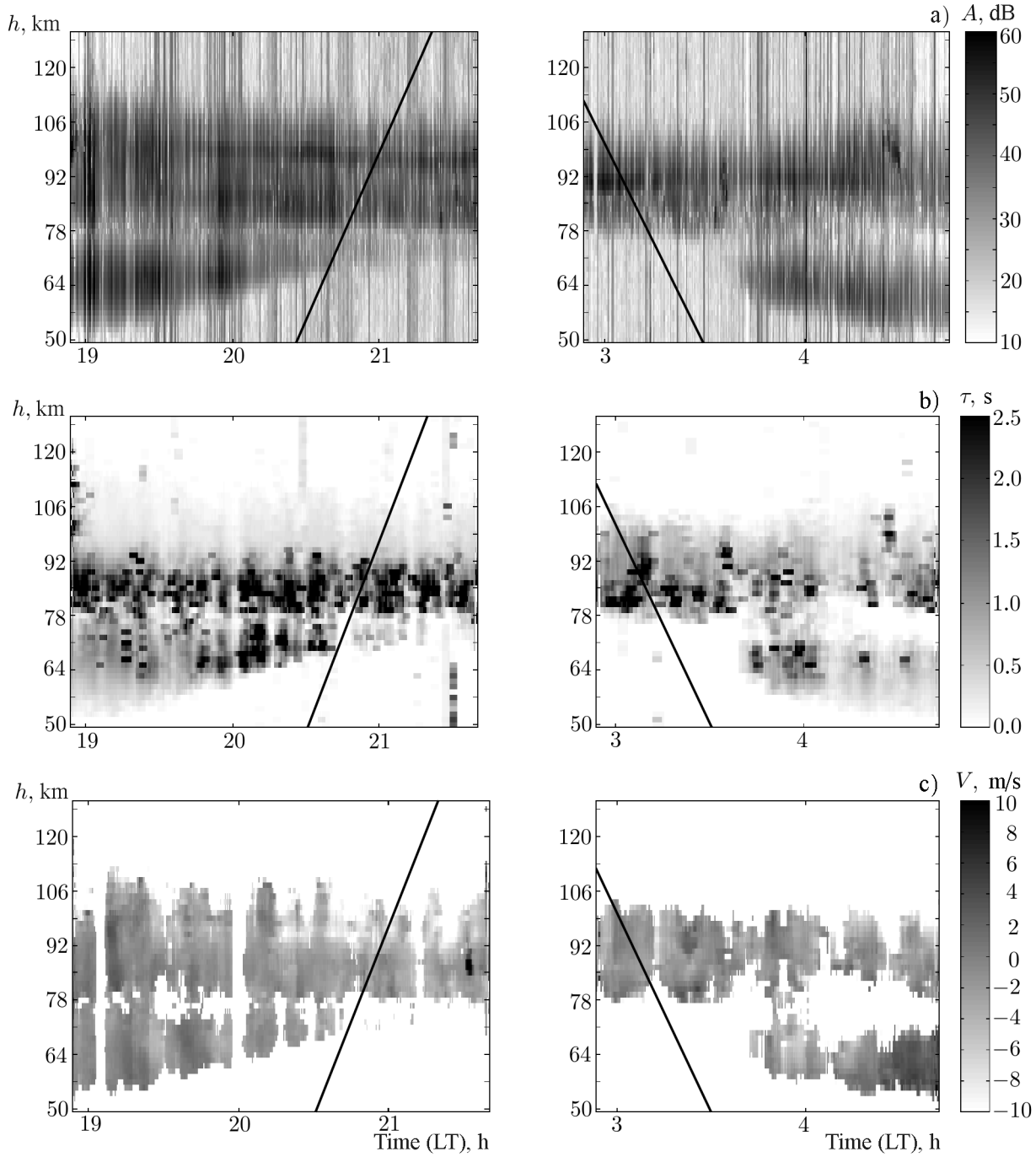


Fig. 2. Brightness records (altitude–time dependences) of the scattered signal for August 16 and 17, 2000: amplitude (*a*), relaxation time (*b*), and velocity of the plasma vertical motion (*c*).

E region. At lower altitudes of 80–86 km, signals from natural large-scale plasma irregularities, i.e., the so-called signals of partial reflections, were presumably observed. Moreover, signals from the $E_s$ layer at altitudes of 105–108 km were observed almost always, i.e., the $E_s$-layer maximum was located at the altitude of the E-layer maximum. The upper sporadic layer, often having a pronounced "cloudy" structure, eventually appeared at the altitude $h \sim 116$ km (Fig. 3). Reflections from the lower boundary of the E region descend to lower altitudes with increasing time, which corresponds to observations of the nighttime electron-density profiles in the E region. Usually, the regular E region and, moreover, the D region are not detected by backscatter radars in the nighttime since the background density decreases by two orders of magnitude,

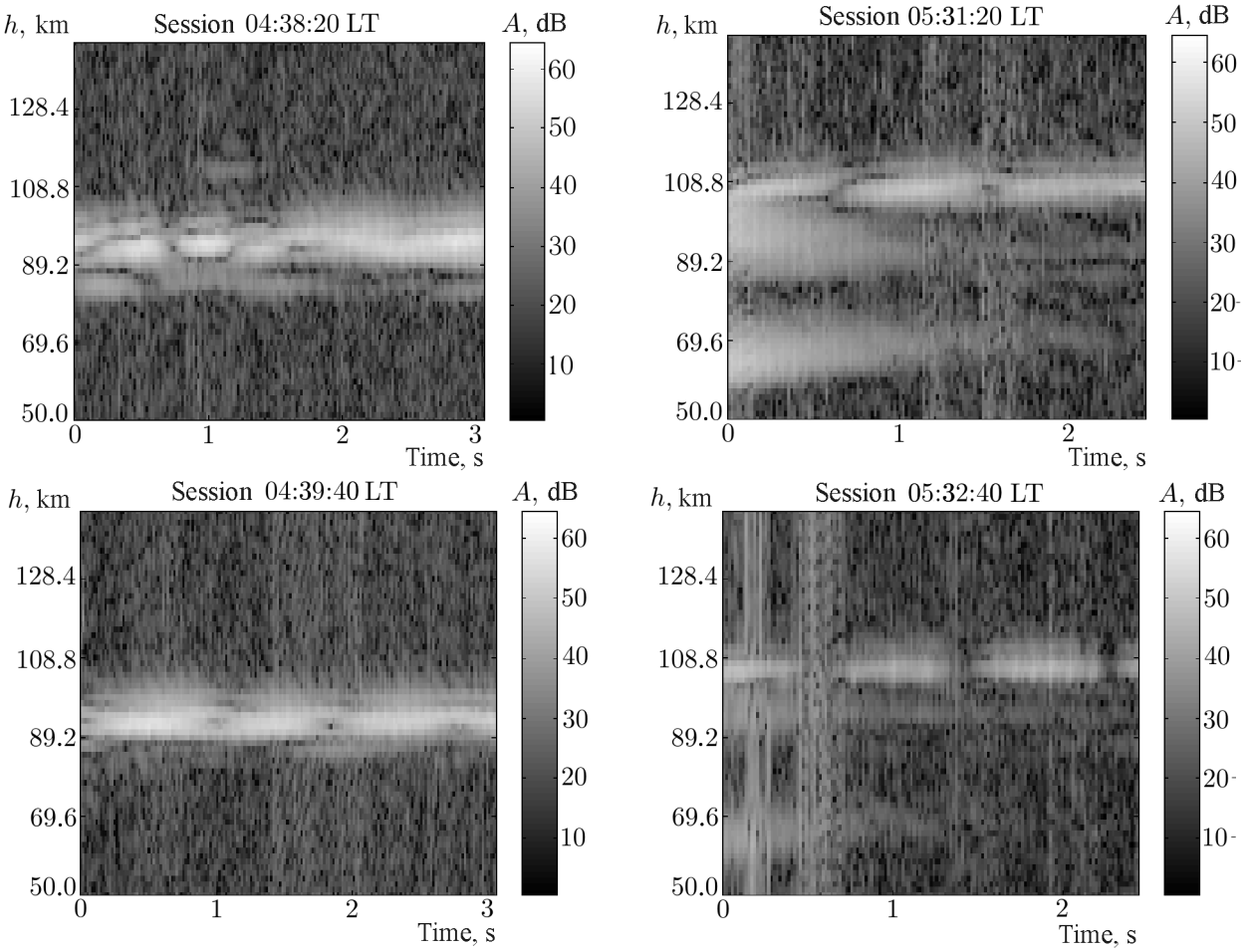


Fig. 3. Examples of brightness records of the amplitude of a signal scattered by the sporadic E layer with a pronounced "cloudy" structure. The data obtained in August 17, 2000 show the underlying layer (left panel) and the $E_s$ layer appeared above the E-region maximum (right panel).

except for the sporadic ionization which can reach and exceed the F-region ionization maximum. It is seen in Fig. 2 that the E layer descends by about 5 km during the night. The E-region altitude begins to increase after the sunrise.

### 3.2. Results of observations in June 15 and 16, 2001

In 2001, the API characteristics were measured during the night between August 15 and 16. Figures 4*a*–4*c* show the brightness records for the amplitudes and relaxation times of signals and for the velocity of the plasma vertical motion in this observation period. Figure 4*d* shows the temporal behavior of the blanketing frequency $f_b$ and the cutoff frequency $f_0$ for the $E_s$ layer as well as the behavior of the cutoff frequencies of the E and F2 layers.

These observations confirm the sunset–sunrise asymmetry of the altitude–time dependence of the scattered signal, which was observed in the previous experiment. Weak signals from APIs in the D region were observed at these altitudes almost till the sunset and appeared in one hour after the sunrise. Generally, their amplitudes were greater at the sunrise. The altitude range occupied by signals from APIs in the D region and the altitude range between the D and E regions, from which these signals were not observed, correspond to observations of 2000.

According to the ionosonde data, a semitransparent $E_s$ layer with the cutoff frequency $f_0 = 5$–$10$ GHz and the blanketing frequency $f_b = 3.0$–$5.5$ MHz was observed from 19:45 LT in June 15 to 03:15 LT in June 16.

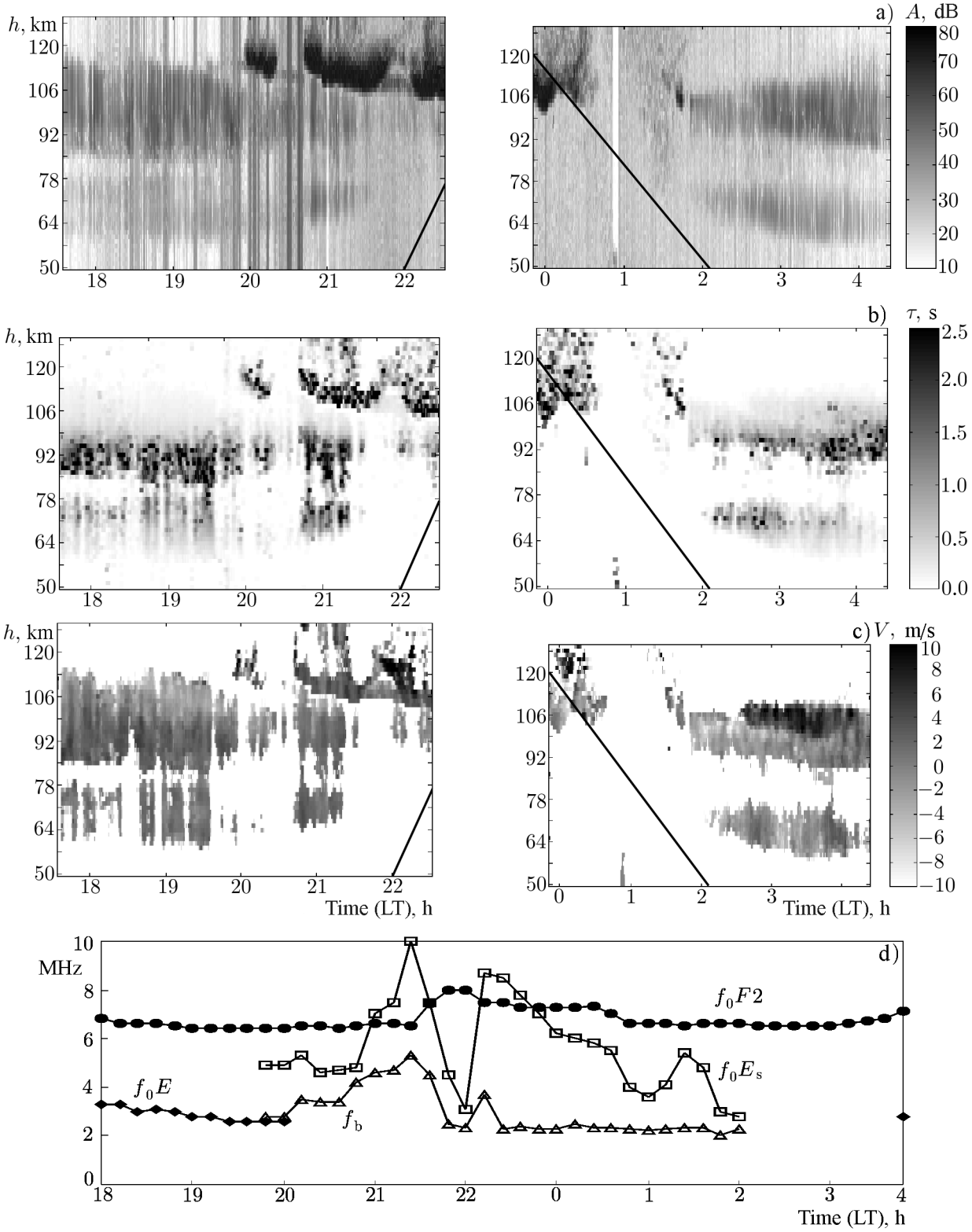


Fig. 4. Altitude-time dependences of the scattered signal for June 15 and 16, 2001: amplitude (*a*), relaxation time (*b*), vertical-motion velocity (*c*), and the temporal behavior of the cutoff frequencies of the ionosphere and the sporadic E layer (*d*).

As a result, up to 5 multiple reflections were registered both in ionograms and during the detection of APIs (Fig. 1*c*).

An interesting feature of the experiment in 2001 is the observation of sporadic structures of several types at the E-layer altitudes. The first type can conventionally be defined as the "classical" long-living $E_s$ layer formed at altitudes of about 95–105 km (the altitudes of the maximum amplitude of a signal from the layer) with a "thickness" of up to 5 km. The thickness is defined as the FWHM range for the scattered-signal amplitude. The amplitude of a signal scattered by APIs from such a layer amounted to 70 dB and the relaxation time reached 10 s.

The sporadic layer of the second type can be called underlying. As a rule, this is a thin layer which was usually observed at an altitude of 85–90 km and often had a well pronounced "cloudy" structure (the sizes of "clouds" are given below). The amplitude of a signal scattered by APIs from such a layer reached 75 dB and its relaxation time, 7–10 s.

Finally, the sporadic layer of the third type is the sequential, or descending layer. Such layers are regularly observed by various methods (see, e.g., [2, 5, 6]). During our experiment, we observed a fairly thick layer with a "thickness" of up to 10 km, scattered-signal amplitude exceeding 75 dB, and relaxation time longer than 10 s. It appeared in ionograms at 19:45 LT in June 15, 2001 and was simultaneously detected by the API method. The layer appeared in the altitude range 113–123 km and gradually descended to altitudes 100–113 km with an effective velocity of about 1 m/s. A wave-like modulation of the descending layer is well seen in Fig. 4*a* (since 8 min in the interval 21:00–22:00 were missed for technical reasons, the time scale after 21:00 is somewhat distorted).

It is seen in the temporal dependences of the cutoff frequencies of the $E_s$ layer on time (Fig. 4*d*) that the frequencies $f_b$ and $f_0$ begin to increase after 21:00 LT and become a factor of 2 greater in 45 min: $f_0$ increases from 4.8 to 10 MHz, and $f_b$, from 3.4 to 5.3 MHz, reaching the maximum value at 21:45 LT. Afterwards, the frequencies of the $E_s$ layer begin to decrease and their deep minima are observed at 22:00 LT. This time interval in Fig. 4*a* corresponds to a sharp decrease in the scattered-signal amplitude and to stratification of the upper descending $E_s$ layer into two thinner layers. An analogous situation also took place from 20:20 to 20:40 LT when the amplitude of the layer reflections decreased from 70 to 40–50 dB and the "thickness" of the layer decreased to 2–3 km. It is interesting that a slight increase in $f_b$ and a small local maximum of $f_0E_s$ were observed at the same time. As far as the F2 layer is concerned, the amplitude of a signal scattered by APIs was constantly high (always greater than 75 dB, i.e., significantly greater than the dynamic range of the receiver), whereas the cutoff frequency of the layer varied weakly near 7 MHz. Only slight (no larger than 1 MHz) variations in the cutoff frequency were observed from 21:45 to 01:00 LT. It is interesting that for almost one hour from 00:45 to 01:30 LT, only the signal from APIs in the F2 region and the "traces" of its numerous multiple reflections (a wide vertical strip in Fig. 4*a*) were registered. Despite the fact that the $E_s$ layer with the cutoff frequency $f_0 \sim 3$–5 MHz and the blanketing frequency $f_b \sim 2.5$ MHz is seen in ionograms at this time, it was registered by the API method only occasionally. This is most probably related to the fact that the directivity pattern of the ionosonde is much wider than that of the "Sura" facility whose radiation forms APIs. Therefore, the ionosonde receives the scattered signal from a much greater area. Since a semitransparent $E_s$ layer is observed in the experiment (Fig. 1*c*) and such layers consist of separate large "clouds" of ionization (a similar example is shown in Fig. 1 in [5]), there could be time intervals when these "clouds" do not fall within the region of the API formation.

At approximately 01:30 LT, signals scattered from the $E_s$ layer near altitudes 113–116 km appeared. Almost simultaneously, signals from APIs in the E region were observed. They were registered till the end of observations. At the same time, reflections from the $E_s$ layer at an altitude slightly lower than that of the E-region maximum are seen in the brightness records.

At the sunrise, the underlying $E_s$ layer was observed more seldom, whereas the layer of "classical" type was registered till almost the end of observations. Possibly, the observed underlying $E_s$ layer is a result of stratification of a layer of "classical" type. Most long-living ions contribute to redistribution of residual ionization in the E region after the sunset. It is also possible that in cases where the underlying $E_s$ layer is observed at the sunrise, both layers, "classical" and underlying, exist all the night, but they are so weak that cannot be detected during a certain time.

## 4. THE SCATTERED-SIGNAL PHASE AND THE VELOCITY OF THE PLASMA VERTICAL MOTION. DYNAMICS OF SPORADIC FORMATIONS

The monograph [4] discusses in detail the fact that APIs are dragged by the moving neutral gas during the relaxation process. Therefore, the registration of the Doppler frequency shift can be used for

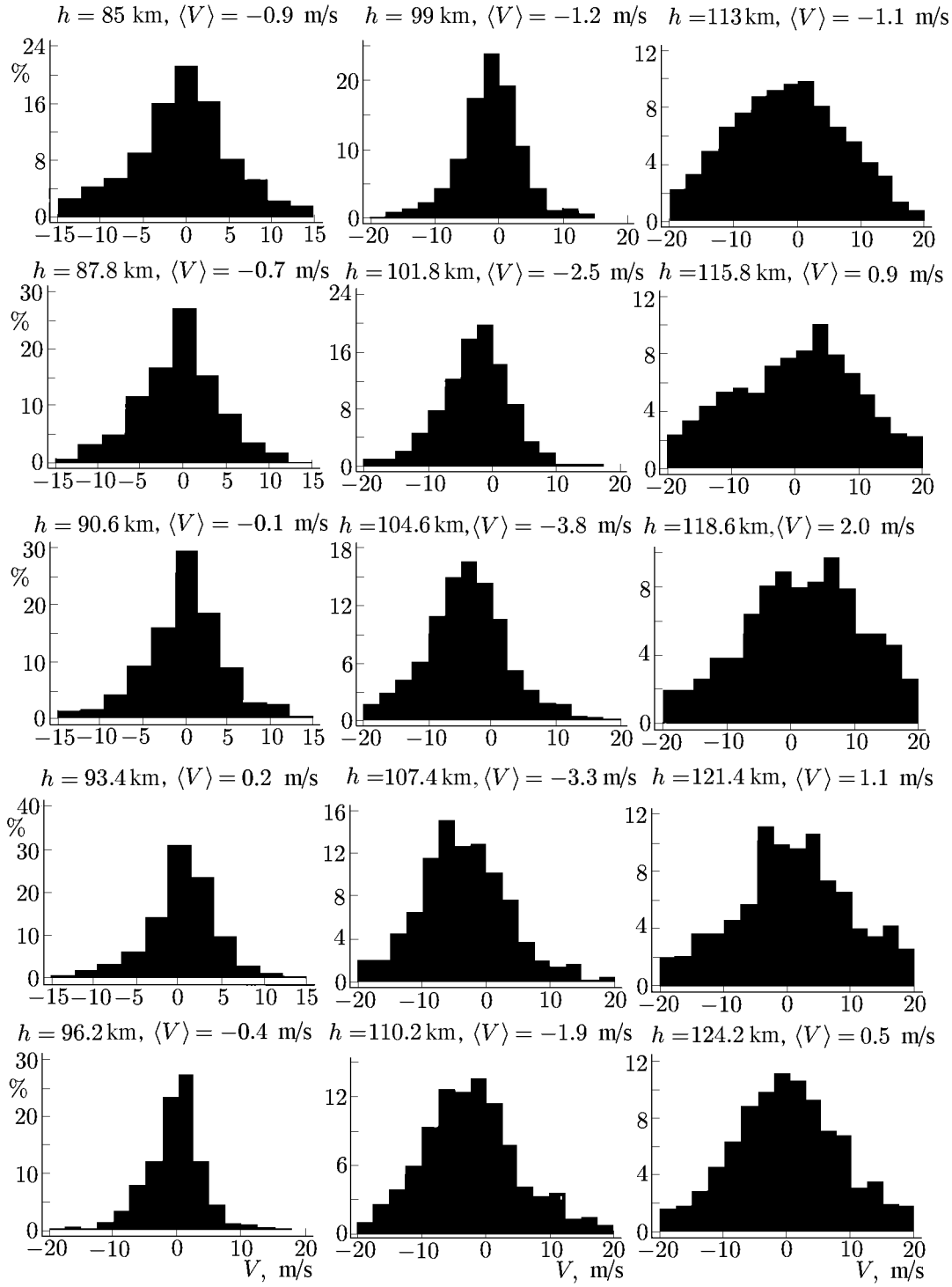


Fig. 5. Histograms of the distribution of the vertical-motion velocity at different altitudes in the evening and night hours in June 15, 2001, The altitude and the average velocity at this altitude are indicated in each histogram.

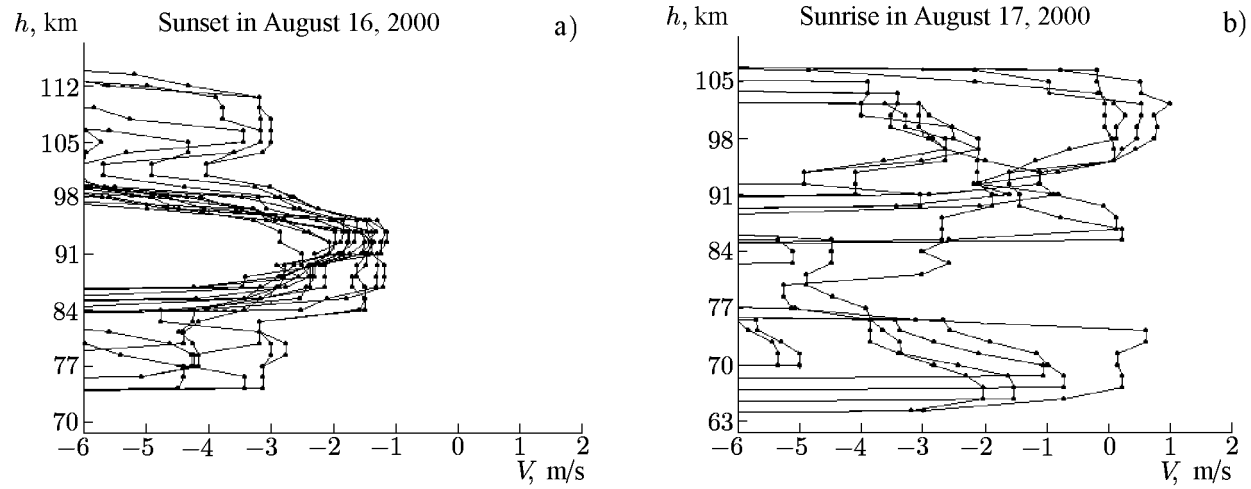


Fig. 6. Altitude profiles of the vertical-motion velocity at the sunrise in August 16, 2000 (*a*) and at the sunset in August 17, 2000 (*b*).

determination of the velocity $V$ of the plasma vertical motion. However, we cannot directly measure the Doppler shift of a signal scattered by APIs since the typical lifetime of inhomogeneities is smaller than the period of Doppler oscillations. This difficulty can be overcome by measuring the scattered-signal phase from which $V$ is then calculated. In this case, the error of determination of $V$, on the average, amounts to 0.05–0.08 m/s [4]. This error can be significant only in the case of strong heating where the frequency of a high-power wave is close to the cutoff frequency of the layer. Under conditions of our experiment, the phase of a signal scattered by APIs varied rapidly in certain time intervals, which caused deep variations in the velocity $V$. Such results are excluded from the analysis. Based on observations of August 2000, most measurements are indicative of the velocities in the range from −10 to 8 m/s with the average value $\langle V \rangle \approx -1$ m/s. It is seen in Fig. 2*c* that the altitude distributions of the vertical velocity in the evening and at the sunrise differ significantly. For example, the velocity in the evening and night hours in both the D and E regions was directed predominantly upward with the shear $\mathrm{d}V/\mathrm{d}h \sim 10^{-5}$–$10^{-3}\,\mathrm{s}^{-1}$ . After the sunrise, the predominant direction of the velocity in the E region varied with a period of 15–20 min, which made it possible to pile up metal ions in the sporadic layer, whereas the predominantly upward motion was observed at the D-region altitudes.

According to observations of 2001, most velocity values lie in the range from −10 to 10 m/s. The vertical velocity at the E-region altitudes, averaged over the entire observation period, ranges from 0.5 to −3.8 m/s at various altitudes.

It is well seen in Fig. 4*c* that the velocities before the sunset in the D region are directed both upward and downward from the ionization region. Downward motion with the negative altitude gradient was observed more frequently near 90 km. Such a gradient should drive ionization to the "underlying" $\mathrm{E_s}$ layer. At the same time, the velocities at the altitudes of the descending sporadic layer were predominantly directed inwards the ionization region.

Variations in the average value and direction of the velocity in the E region can be seen in the histograms of the altitude distribution of $V$ for altitudes 85–124.2 km. These histograms are shown in Fig. 5 for the evening time of June 15, 2001. For each histogram, the altitude and the average vertical velocity $\langle V \rangle$ at this altitude are indicated. At altitudes of about 92 and 114 km, the average velocity reversed sign, i.e., the sporadic E layer could be formed due to the wind-shear mechanism of pile-up of positive ions. The velocities averaged over the entire period are small in magnitude. However, in particular sessions, they were significant and had the direction necessary for the pile-up. Here, we only give the average values since we do not analyze the vertical-velocity variations in detail. However, it is seen even from average values that the $\mathrm{E_s}$ layer could be formed at altitudes 92 and 114 km due to the pile-up of metal ions. Note that the sporadic layers were observed at exactly these altitudes.

The vertical-velocity shears at altitudes 100–113 km, determined from the altitude profiles $V(h)$, amount to $|\mathrm{d}V/\mathrm{d}h| \approx 5 \cdot 10^{-5}$–$10^{-4}\,\mathrm{s}^{-1}$. Such shears are sufficient for the formation of the $\mathrm{E_s}$ layer due to the pile-up of long-living metal ions. In many cases, the maximum amplitude of a signal from the $E_\mathrm{s}$ layer was observed at an altitude at which $V \sim 0$, as well as at altitudes with velocity shear sufficient for the pile-up. According to estimates given in [1], the pile-up of ions can occur even for shears of about $5{\cdot}10^{-4}$ $\mathrm{s}^{-1}$.

The features of the sunset–sunrise change in the dynamic regime of the ionosphere are manifested in an altitude variation in the vertical velocity. This variation is illustrated by Fig. 6 showing several successive profiles $V(h)$ for the intervals including the sunset and the sunrise in the E region. It is seen that the altitude dependences $V(h)$ have an obvious wave-like form with an altitude period of about 15 km.

## 5. THE INFLUENCE OF THE $\mathrm{E_S}$ LAYER ON THE AMPLITUDE AND RELAXATION TIME OF THE SCATTERED SIGNALS. METAL IONS

The influence of the $\mathrm{E_s}$ layer on the scattered-signal amplitude $A$ consists in a significant increase in the amplitude (sometimes by 30–40 dB) observed in the dependence $A(h)$ due to an increase in the electron number density in the layer and an increase in the reflection coefficient. It is evident that the relaxation time should also increase.

Without allowance for atmospheric turbulence, which is valid at altitudes above the turbopause, we can assume that the relaxation of irregularities in the E region is stipulated by ambipolar diffusion [4]. In this case, the altitude dependence of the API relaxation time $\tau(h)$ is exponential if the $\mathrm{E_s}$ layer is absent. The effect of turbulence leads to a decrease in the relaxation time compared with the time of diffusion spreading of APIs [4]. If the $\mathrm{E_s}$ layer exists at a certain altitude, then local maxima are observed in the dependence $\tau(h)$ for this altitude. At the maxima, $\tau$ sometimes increases by several times. This is explained by the fact that an increase in electron number density in the $\mathrm{E_s}$ layer compared with the background density in the E region leads to a decrease in the refractive index, an increase in the wavelength in the layer, and an increase in the time of diffusion spreading of inhomogeneities. In this case, the relative variation in $\tau$ is given by the formula

$$\delta\tau = \frac{\Delta\tau}{\tau} = \frac{1}{2}\,\frac{\Delta n}{n}\,, \tag{1}$$

whereas the relative variation in the plasma frequency of the $\mathrm{E_s}$ layer with respect to the background value in the E region is written as [4]

$$\delta f_0 = \frac{f_0 E_\mathrm{s}}{f_0 E} = \frac{1}{2}\delta\tau\left[\frac{f\,(f - f_\mathrm{L})}{(f_0 E)^2} - 1\right], \tag{2}$$

where $f_0 E_\mathrm{s}$ and $f_0 E$ are the plasma frequencies of the $\mathrm{E_s}$ layer and the E region, respectively, $f_\mathrm{L} = f_H \cos\theta$, $f_H$ is the electron gyrofrequency, $\theta$ is the angle between the geomagnetic field and the wave vector of a radio wave, $\Delta\tau$ is the relaxation-time increment at the $\mathrm{E_s}$-layer altitude with respect to the diffusion time, $\tau$ is the diffusion relaxation time in the E region in the absence of the sporadic layer, $n$ is the refractive index at a given altitude, and $\Delta n$ is the refractive-index change due to the effect of the $\mathrm{E_s}$ layer. Substituting the values $f = 5.67$ MHz, $f_0 E = 3.5$–$4.0$ MHz, $f_\mathrm{L} = 1.3$ MHz, and $\delta\tau = 0.1$–$0.5$ into Eq. (2), we obtain $\delta f_0 = 0.03$–$0.25$. Thus, even moderately intense layers significantly increase the API relaxation time.

Another factor causing an increase in the API relaxation time is the presence of long-living metal ions at these altitudes. In accordance with the wind-shear theory, these ions are piled up in narrow layers. This leads to the formation of the $\mathrm{E_s}$ layer at mid-latitudes [2]. Meanwhile, the diffusion time $\tau$ of API relaxation is proportional to the relative molecular mass $M$ of predominant ions and is given by the formula

$$\tau = \frac{1}{K^2 D_\mathrm{a}} = \frac{M\nu_\mathrm{in}}{k\,(T_\mathrm{e0} + T_\mathrm{i0})\,K^2}\,, \tag{3}$$

where $k$ is Boltzmann's constant, $K = 4\pi/\lambda$ is the wave number of the standing wave, $\lambda = \lambda_0/n$ is the

wavelength in the medium, $D_\mathrm{a}$ is the ambipolar diffusion coefficient, $M$ is the relative molecular mass of ions, $T_\mathrm{e0}$ and $T_\mathrm{i0}$ are the unperturbed electron and ion temperatures, respectively, and $\nu_\mathrm{in}$ is the rate of ion collisions with neutral molecules.

According to the results of spectrometric measurements (see, e.g., [7, 8]), metal ions $Fe^+$ ($M = 56$), $Mg^+$ ($M = 24$), $Ca^+$ ($M = 40$), $Al^+$ ($M = 27$), $Na^+$ ($M = 22$), and $Si^+$ ($M = 28$) were detected in sporadic layers. It immediately follows from Eq. (3) that the iron ions with the atomic mass $M = 56$, which is almost two times greater than the average molecular mass of the atmospheric ions $NO^+$ ($M = 30$) and $O_2^+$ ($M = 32$), predominant at the E-region altitudes, or the calcium-ion mass $M = 40$, should affect $\tau$ most significantly. Measurements show that heavy ions can constitute up to 80% of the total amount of metal ions in the $E_s$ layer [7–12]. In this case, one can expect a considerable increase in $\tau$ at the sporadic-layer altitudes. If the cutoff frequencies of the $E_s$ layer and the E region are known, then, using Eqs. (1) and (3), one can estimate the influence of both the refractive index $n$ and the relative molecular mass $M$ of metal ions on the relaxation time of the scattered signal:

$$\frac{\tau_{E_\mathrm{s}}}{\tau} = \left(\frac{n_E}{n_{E_\mathrm{s}}}\right)^2 \left(\frac{M_\mathrm{m}}{M_\mathrm{a}}\right). \tag{4}$$

Here, $M_\mathrm{m}$ and $M_\mathrm{a}$ are the relative masses of metal and atmospheric ions, respectively.

Thus, by measuring $\Delta\tau/\tau$ or $\tau_{E_\mathrm{s}}/\tau$ in the experiment, one can estimate the relative molecular mass of metal ions.[1]

During measurements from 19:45 to 20:45 LT in June 15, 2001, it was found that $\Delta\tau/\tau \approx 1.0$–$1.8$. Taking $f_0E = 2.5\,\mathrm{MHz}$, $f_\mathrm{b} = 3$–$3.5\,\mathrm{MHz}$, and $f = 5.67\,\mathrm{MHz}$, we obtain the relative molecular masses 39 and 57 that are close to the masses of the $Ca^+$ and $Fe^+$ ions, respectively, which seems rather plausible. At the same time, $f_0E = 2.0\,\mathrm{MHz}$, $f_\mathrm{b} = 2.2\,\mathrm{MHz}$, and $\Delta\tau/\tau \approx 0.3$ for the "classical" $E_s$ layer observed before the sunset at altitudes 95–105 km, whence we obtain $M_\mathrm{m} = 37$ for the ion mass.

According to the ionospheric data for observations in August 16 and 17, 2000, the cutoff frequency of the E layer was almost equal to the blanketing frequency of the $E_s$ layer. In this case, an increase in the API relaxation time should be determined only by the mass of metal ions. It is typical that in that time, variations in $\tau$ amount to 30–50% in most sessions, which yields the values 37–42 for $M_\mathrm{m}$.

The total number density of all metal ions at the altitude of the $E_s$-layer maximum can also be estimated if we use a calculation method proposed in [13, 14]. This method is based on measuring the velocity of the plasma vertical motion by using the API method and the vertical-sounding data. The analysis begins with the steady-state continuity equation for electrons in the approximation of the plane-layered ionosphere. The weighted-mean value of the recombination rates of various positive ions, which are present at the E-region altitudes, is used as the effective recombination rate $\alpha$. We also assume that the $E_s$ layer does not affect the function describing generation of electrons. Thus, we obtain that the number density of the atmospheric ($NO^+$ and $O_2^+$) and metal ions depend on the altitude shear $\mathrm{d}V/\mathrm{d}h$ of the vertical velocity and the electron number density $N_\mathrm{s}$ in the $E_s$-layer maximum and are determined by the formulas [15]

$$\alpha = \alpha_0 \left(\frac{N_0}{N_\mathrm{s}}\right)^2 - \frac{1}{N}\frac{\mathrm{d}V}{\mathrm{d}h}, \quad N_\mathrm{a} = N_\mathrm{s}\left(\frac{\alpha}{\alpha_0}\right) = \frac{N_0^2}{N_\mathrm{s}} - \frac{1}{\alpha_0}\frac{\mathrm{d}V}{\mathrm{d}h}, \quad N_\mathrm{m} = N_\mathrm{s}\left[1 - \left(\frac{N_0}{N_\mathrm{s}}\right)^2\right] + \frac{1}{\alpha_0}\frac{\mathrm{d}V}{\mathrm{d}h}, \tag{5}$$

where $\alpha$ is the effective recombination rate, $\alpha_0 = 4.4\cdot10^{-7}\,(300/T_\mathrm{e}[\mathrm{K}])\,\mathrm{cm}^3/\mathrm{s}$, $T_\mathrm{e}$ is the electron temperature

[1] Strictly speaking, this method allows one to estimate the effective mass of ions present in the ionosphere at the altitude of the $E_s$-layer maximum. This mass is expressed as $M_\mathrm{eff} = N^{-1}(\Sigma_{i=1}^n M_{\mathrm{m}i}N_{\mathrm{m}i} + \Sigma_{j=1}^k M_{\mathrm{a}j}N_{\mathrm{a}j})$, where $N_{\mathrm{m}i}$ are the number densities of various metal ions and $N_{\mathrm{a}j}$ are the number density of atmospheric ions. The total ion number density $N$ is equal to the electron number density $N_\mathrm{e}$ within the framework of the approximation of quasi-neutral plasma. It is known that a sharp decrease in the content of atmospheric ions compared with the background values is observed in the $E_s$ layer. As a result, the quantity $M_\mathrm{eff}$ differs from the mass of predominant ions by no larger than 3–5%.

at the altitude of the $E_s$-layer maximum, also determined by the API method [4], $N_a$ and $N_m$ are the number densities of the atmospheric and metal ions, respectively, and $N_0$ and $N_s$ are the electron number densities in the E region and at the altitude of the $E_s$-layer maximum, respectively. Thus, using the velocity $V$ of the plasma vertical motion, measured by the API method, and the frequency characteristics of the $E_s$ layer and the E region from the vertical-sounding data, the effective recombination rate and the number densities of atmospheric and metal ions can be determined from Eq. (5).

Estimates made for the two above-mentioned cases yield $N_m \sim 10^4\,\mathrm{cm}^{-3}$ and $N_a \sim 8 \cdot 10^4\,\mathrm{cm}^{-3}$ for the layer descending from the altitude 113 km (at the descent beginning) and $N_m \sim 7.3 \cdot 10^3\,\mathrm{cm}^{-3}$ and $N_a \sim 5.3 \cdot 10^4\,\mathrm{cm}^{-3}$ for the layer whose maximum is located at an altitude of about 100 km. Unfortunately, we were not able to make such estimates for the entire time of observation of the descending $E_s$ layer since the ionosonde did not register the low electron number density in the E region during the night (Fig. 4*d*). As a result, the data on $f_0E$ are absent.

Let us compare the obtained results with the data of measurements given in the literature for the altitude distribution of metal ions at the altitude of the sporadic E layer.

During the last thirty years, rocket spectrometric measurements and then lidar measurements at various altitudes gave a rather complete picture of distribution of metal ions and the basic atmospheric ions $NO^+$ and $O_2^+$ in the altitude range 80–120 km [7–12], including the periods of observations of meteor trails. From the data presented in [11] for 30°–55° N, one can conclude that three basic local maxima determining the $E_s$-layer altitudes exist in the altitude distribution of metal ions. One maximum in the range 90–95 km with the total number density of all metal ions up to $N_m \sim 2 \cdot 10^4\,\mathrm{cm}^{-3}$ is related to the layers consisting mainly of the ions $Fe^+$ (up to $6 \cdot 10^3\,\mathrm{cm}^{-3}$), $Mg^+$ (up to $4 \cdot 10^3\,\mathrm{cm}^{-3}$), $Na^+$ (up to $7 \cdot 10^2\,\mathrm{cm}^{-3}$), and $Ca^+$ (up to $2 \cdot 10^2\,\mathrm{cm}^{-3}$). Another maximum near the altitude 105 km with total number density of all metal ions up to $N_m \sim 10^5\,\mathrm{cm}^{-3}$ is related to the layers of the same metal ions, although the ions $Si^+$ ($M = 28$) are sometimes registered. The number density of the silicon ions can be comparable with or even exceed that of the iron ions. Finally, the third density maximum of metal ions with $N_m \sim 2 \cdot 10^4\,\mathrm{cm}^{-3}$ is observed in many cases at altitudes 113–115 km. In a number of measurements, ion layers with a high content of $Na^+$ (up to $4 \cdot 10^3\,\mathrm{cm}^{-3}$) were registered. As rule, the altitudes of the maximum number densities of various ions differ by 1–2 km.

Comparing our estimates with the above results of direct measurements, we can conclude that the total number density of metal ions, obtained from Eq. (5), agrees well with the results of lidar and rocket measurements.

Having the data of direct measurements of the ion content, we can estimate the number density of ions of a certain type. For example, according to the data given in [12, 15], the number density of the $Fe^+$ ions amounts to about 55% of the total number density of metal ions at altitudes 113–115 km, whereas the number density of the calcium ions was much smaller, from 0.5 to 5%. At altitudes 95–100 km, the number density of the $Ca^+$ ions usually does not exceed 5–10% of that of the $Fe^+$ ions. If we adopt that the fraction of the $Fe^+$ ions is of the order of 50%, then, for the total number density $N_m \sim 10^4\,\mathrm{cm}^{-3}$ of all ions, the number density of the iron ions amounts to $N_m(Fe^+) \sim 5 \cdot 10^3\,\mathrm{cm}^{-3}$, which does not contradict the results of direct measurements.

The performed comparison shows that the proposed method is promising for studying the ion content at the altitudes of the sporadic E layer.

It was noted above that the API method allows us to determine most exactly the types of metal ions whose masses exceed the masses of basic atmospheric ions. In this respect, the method needs to be improved to identify lighter, but not less significant ions in the $E_s$ layer, e.g., the $Na^+$ and $Mg^+$ ions, whose number densities can be much greater than that of $Fe^+$ in the $E_s$ layer.

Thus, the type of relatively heavy meteor ion contributing to the formation of the $E_s$ layer and to the total number density of all metal ions can be determined on the basis of the altitude dependence of the API relaxation time, the velocity shear of the vertical motion of the ionospheric plasma, and the vertical-sounding data.

## 6. INTERNAL GRAVITY WAVES AND THE FORMATION OF THE $E_S$ LAYER. PARAMETERS OF IRREGULARITIES IN THE $E_S$ LAYER

Within the framework of the wind-shear theory, narrow sporadic layers of ionization are formed in the mid-latitude ionosphere due to the vertical shear of the horizontal velocity of the plasma or the horizontal

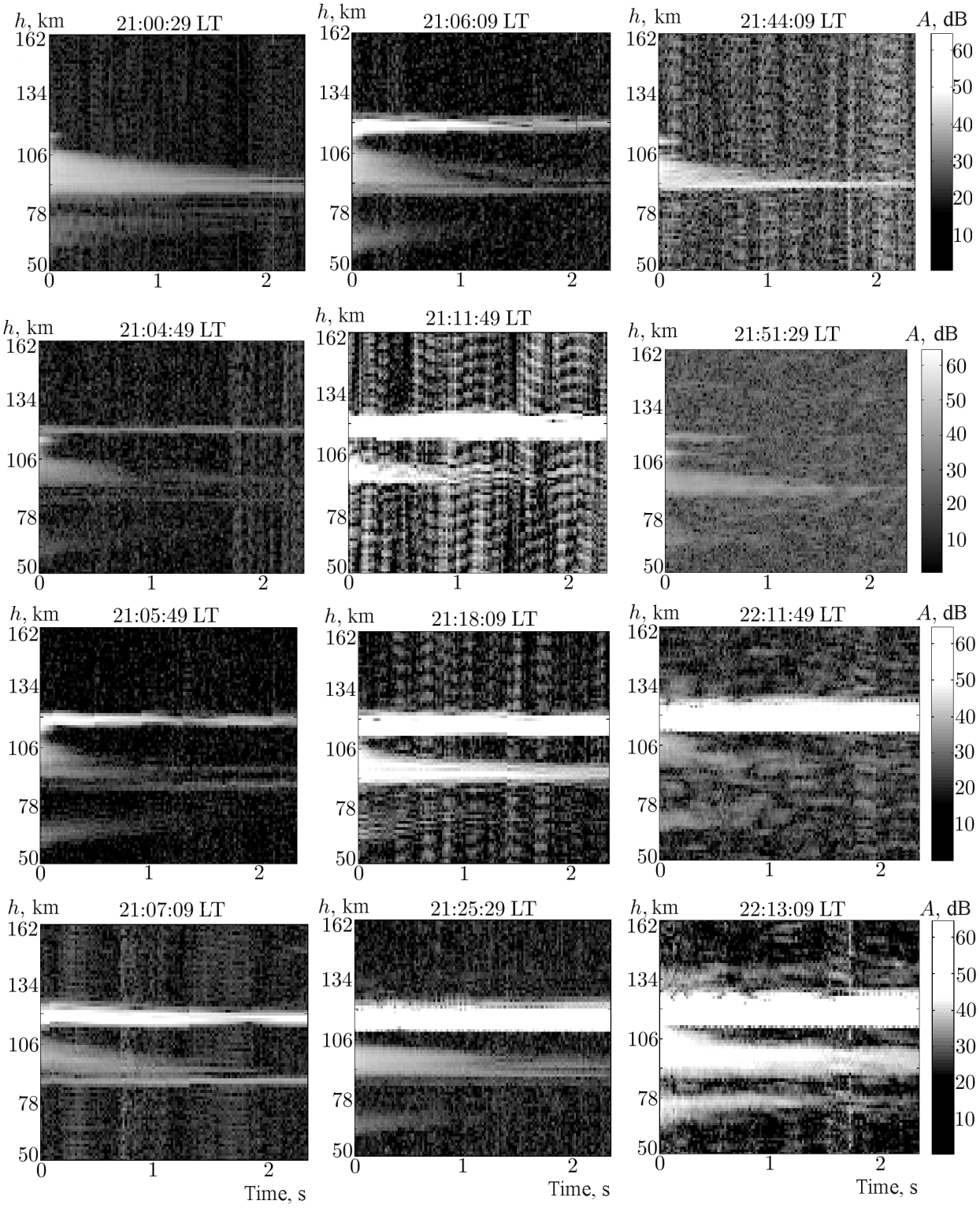


Fig. 7. Formation of the sporadic E layer at the sunset in June 15, 2001.

wind since the plasma is an admixture and moves with the neutral-wind velocity in the lower ionosphere. This causes vertical transport of the plasma. The wind shear necessary for the plasma pile-up can in particular be created by the propagation of intense internal gravity waves [2, 5, 6]. There is no doubt that the internal gravity waves are excited at the time when the solar terminator passes through the observation point, i.e., at the sunset and the sunrise [14, 16, 17].

In the literature (see, e.g., review papers [2, 6]), numerous data have been reported on the $E_s$-layer observations and their relation to internal gravity waves, tides, and traveling ionospheric disturbances. The problem of appearance of the horizontal-wind shears created by internal gravity waves and required for the formation of the $E_s$ layer has been considered theoretically. According to our measurements by the API method of the velocities of the plasma vertical motion and of the electron density profiles in the lower ionosphere in 1990–1991, the results of which are presented in detail in [4], the internal gravity waves essentially determine the features of altitude variations in the vertical velocity.

The spectral analysis of the amplitude and relaxation time of the scattered signal as well as of the vertical velocity at the E-region altitudes for the measurement results of June 2001 reveals wave-like variations in these parameters with the most typical periods equal to 15, 30, 120, and 240 min. The period corresponding to the Brunt–Väisälä frequency, at which the spectrum sharply decreases, amounts to 6.5 to 8.5 min. Based on the simultaneous measurements of the scattered signal characteristics in a wide altitude range, it is possible to elucidate variations in the phase velocity of the wave, which is predominantly downward-directed. An altitude period of about 15 km was identified in the altitude profiles of the vertical velocity. We can assume that the propagation of intense internal gravity waves during observations in June 15 and 16, 2001 can give rise to wind shears of the vertical velocity, which are required for the formation of the descending sporadic E layer. Such an interpretation is additionally supported by the presence of deep variations in the cutoff frequencies of the layers (Fig. 4*d*) during the observation of the descending $E_s$ layer.

Figure 7 shows an interesting feature of the formation of the $E_s$ layer before the sunset in June 15, 2001. Slightly below the altitude 115 km at which the $E_s$ layer is formed later, one can see another layer. The amplitude of a signal scattered by this layer is close to that of a signal from APIs in the E region. However, the relaxation time of this layer is significantly smaller. It is seen is successive snapshots how the $E_s$ layer develops. Its intensity significantly increases with time and it merges with the above-mentioned small layer. The $E_s$ layer weakens within approximately 30 min and then the process repeats. Note that the small layer does not disappear. The origin of such long-living layers cannot be explained unambiguously. We can only assume that these layers appear as a result of stratification of the regular E layer [4].

It was noted above that sporadic formations, especially underlying layers, have a well pronounced "cloudy" structure, and the signal amplitude at the "cloud" center can be 10–40 dB higher than at the boundaries. According to a theory of the formation and relaxation of APIs in the E region, considered in detail in [4], the scattered-signal amplitude is proportional to the electron number density in an inhomogeneity, i.e., the above-mentioned variation in $A$ corresponds to a relative number density of up to $\delta N \sim 10^2$.

The sizes of "clouds" can be roughly estimated as $l = V_0\xi$, where $V_0$ is the horizontal velocity of motion of the "clouds" and $\xi$ is their duration. Putting $V_0 \sim 100$ m/s, we obtain the scales $l \sim 50$–200 m and $l \sim 150$–300 m from the measurement results of 2000 and 2001, respectively. Thus, we can assume that the observed clouds of ionization are fairly intense mid-scale irregularities. Similar results were obtained in [1] from the data of daytime measurements in August 1999.

## 7. CONCLUSIONS

In this paper, we presented the results of studying the sporadic layers of ionization in the lower ionosphere by the method of backscattering of radio waves from artificial periodic inhomogeneities of the ionospheric plasma on the basis of observations at the sunset–sunrise time in the summer months of 2000 and 2001. Measurements were carried out at the "Sura" heating facility of the Radiophysical Research Institute (Nizhny Novgorod, Russia). Based on the analysis of the altitude–time dependences of the scattered-signal

parameters, we obtained new data on the formation and dynamics of the mid-latitude sporadic E layer in the evening and night time. At the E-region altitudes, sporadic formations of various types were observed. The simultaneous measurements of the amplitude, the relaxation time, and the velocity of the vertical motion of the ionospheric plasma allowed us to study the altitude profiles and the temporal behavior of these characteristics and to estimate the wave-motion parameters at these altitudes.

We discussed the role of internal gravity waves in the formation of the descending $E_s$ layer. It was revealed that the "classical" $E_s$ layers for which the altitude of the layer maximum is close to that of the E-region maximum are observed most often. The features of the sunset–sunrise variations in the scattered-signal characteristics were studied and the relative molecular mass and the total number density of metal ions in the layer were estimated. In particular, it was found that the observed variations in the API relaxation time can be caused by sporadic layers comprising the calcium and iron ions and having the total number density of all metal ions up to $7.3 \cdot 10^3$–$10^4\,\mathrm{cm}^{-3}$ at altitudes 100–115 km.

This work was supported by the Russian Foundation for Basic Research (project Nos. 01–05–65025 and 02–05–65281). The work of L. M. Kagan was supported in part by the Canadian Natural Sciences and Engineering Research Council.

**REFERENCES**

1. N. V. Bakhmet'eva, V. V. Belikovich, E. A. Benediktov, and A. V. Tolmacheva, *Radiophys. Quantum. Electron.*, **44**, No. 12, 924 (2001).
2. J. D. Whitehead, *J. Atmos. Terr. Phys.*, **51**, No. 5, 401 (1989).
3. V. V. Belikovich and E. A. Benediktov, *Radiophys. Quantum. Electron.*, **45**, No. 6, 458 (2002).
4. E. A. Benediktov, V. V. Belikovich, A. V. Tolmacheva, and N. V. Bakhmet'eva, *Study of the Ionosphere by Using Artificial Periodic Inhomogeneities* [in Russian], Inst. Appl. Phys., Nizhny Novgorod (1999).
5. L. M. Kagan, N. V. Bakhmet'eva, V. V. Belikovich, et al., *Radio Sci.*, **37**, No. 6, 1106 (2002).
6. B. N. Gershman, Yu. A. Ignat'ev, and G. Kh. Kamenetskaya, *Mechanisms of the Sporadic-Layer Formation at Various Latitudes* [in Russian], Nauka, Moscow (1976).
7. R. S. Narcisi and A. D. Bailey, *J. Geophys. Res.*, **70**, 3687 (1965).
8. R. S. Narcisi, A. D. Bailey, L. E. Wlodyka, and C. R. Philbrick, *J. Atmos. Terr. Phys.*, **34**, 647 (1972).
9. J. D. Mathews, *J. Atmos. Solar-Terr. Phys.*, **60**, No. 4, 413 (1998).
10. S. Kumar and W. B. Hanson, *J. Geophys. Res.*, **85**, 6783 (1980).
11. A. Huuskonen, T. Nygren, L. Jalonen, et al., *J. Geophys. Res.*, **93**, 14603 (1988).
12. J. M. Grebovsky, R. A. Goldberg, and W. D. Pesnall, *J. Atmos. Solar-Terr. Phys.*, **60**, 607 (1998).
13. N. V. Bakhmet'eva, V. V. Belikovich, Yu. A. Ignat'ev, and A. A. Ponyatov, *Geomagn. Aeron.*, **36**, No. 6, 756 (1996).
14. N. V. Bakhmet'eva, V. V. Belikovich, Yu. A. Ignat'ev, and A. A. Ponyatov, *Radiophys. Quantum. Electron.*, **42**, No. 1, 22 (1999).
15. M. Gerding, M. Alpers, J. Hoffner, and U. Von Zahn, *Ann. Geophys.*, **19**, No. 1, 47 (2001).
16. V. M. Somsikov, *Solar Terminator and Dynamics of the Atmosphere* [in Russian], Nauka, Alma-Ata (1983).
17. K. Hocke and K. Schlegel, *Ann. Geophys.*, **14**, No. 9, 917 (1996).